Geometric Interactions in Binary Colloidal Dispersions

P. Bartlett* and R. H. Ottewill

School of Chemistry, Cantock's Close, Bristol University, Bristol BS8 1TS, England

Received February 3, 1992. In Final Form: May 6, 1992

Small-angle neutron scattering experiments were performed on concentrated binary dispersions of sterically-stabilized poly(methyl methacrylate) particles of size ratio ~0.31 dispersed in a mixture of *cis*-decalin-h_{18} and octane-d_{18}. Using a contrast match technique, we have, for the first time, studied the local structure of small spheres in a simple (hard-sphere) colloidal mixture. In particular, our experiments demonstrate that the small spheres show evidence of particle clustering. We show that this observation is in accord with a long-ranged attractive force between the small spheres resulting from the depletion of larger particles from between the surfaces of the small spheres.

1. Introduction

A major factor controlling the stability and flow properties of colloidal dispersions is the state of aggregation of the colloidal particles. In a binary mixture of particles, A and B, the averaged microstructure may reflect either a tendency toward *dispersion*, in which an A species will have on average both A and B particles as neighbors, or *association* in which separate clusters of A and B form. A key feature of mixtures is that the relationship between the local structure and the interparticle potential is much more subtle than for the one-component case. Simple considerations show,[1] for example, that there is always an *effective* attraction between particles of the same species in a binary mixture. In particular, an effective attractive interaction may arise in a mixture in which the component interaction potentials are themselves purely repulsive. Probably the best known example of this phenomenon is the *depletion* flocculation which occurs when a small amount of a free (nonadsorbing) polymer is added to an initially stable colloidal dispersion.[2] The physical basis for this polymer-induced clustering has been qualitatively explained by a simple excluded-volume model first proposed by Asakura and Oosawa (AO)[3,4] and later extended by Vrij[5] to treat phase separation in these mixtures.

In the AO model the polymer molecules and the colloidal particles are represented by a mixture of hard spheres of diameters σ_p and σ_c, respectively. However while the polymer molecules behave like hard spheres toward the colloidal particles, they are assumed to be free to interpenetrate each other such that the pair potentials have the normal hard-sphere form

$$u_{ij}(r) = \begin{cases} \infty & \text{if } r < \sigma_{ij} \\ 0 & \text{otherwise} \end{cases} \tag{1}$$

but with nonadditive interaction diameters given by

$$\sigma_{cc} = \sigma_c$$

$$\sigma_{pp} = 0$$

$$\sigma_{pc} = (\sigma_p + \sigma_c)/2 \tag{2}$$

Since the cross-interaction diameter is finite, the centers of the small (polymer) spheres are excluded from a spherical shell around each colloidal particle (see Figure 1). When two of the large spheres are close together, the volume inaccessible to the centers of the smaller spheres is smaller than when the particles are far apart (the difference is shown by the solid area in Figure 1). The result is an *effective* attractive potential which drives the two large (colloidal) spheres together. The form of this *depletion* potential is[3-5]

$$V_{cc}(r) = \begin{cases} \infty & \text{for } r < \sigma_c \\ -\frac{4}{3}\pi n_p kT\left[\sigma_{pc}^3 - \frac{3}{4}r\sigma_{pc}^2 + \frac{1}{16}r^3\right] & \text{for } \sigma_c < r < 2\sigma_{pc} \\ 0 & \text{otherwise} \end{cases} \tag{3}$$

where n_p is the polymer number density. From the physical picture for the depletion interaction in Figure 1, it is apparent that the same arguments are applicable (at least in the limit of low densities, see below) to a mixture of hard spheres where in contrast to the AO model the diameters are additive, i.e. $\sigma_{ij} = (\sigma_{ii} + \sigma_{jj})/2$. The depletion mechanism in such a hard sphere mixture has been described by Biben and Hansen.[6] In the framework of the Percus–Yevick theory Biben and Hansen showed that there is an effective attraction between the larger spheres of diameter σ_{ii} in a mixture when their mutual separation is in the range $\sigma_{ii} < r < \sigma_{ii} + \sigma_{jj}$; here σ_{jj} is the small sphere diameter. In this article we describe experimental evidence for the existence of this depletion force in an asymmetrically sized mixture of colloidal particles.

In this work, the structure of a bimodal mixture of spheres of size ratio ~0.31 was studied with small-angle neutron scattering (SANS) measurements. Our experiments were designed to probe the local organization of the small spheres which, arguments outlined in section 2 indicate, should be most strongly influenced by depletion interactions. To emphasize the small sphere microstructure, we have used a contrast matching technique. Large hydrogenated poly(methyl methacrylate) (PMMA) spheres

* Author for correspondence.

(1) Israelachvili, J. N. *Intermolecular and Surface Forces*; Academic Press: London, 1985.
(2) Napper, D. H. *Polymeric Stabilization of Colloidal Dispersions*; Academic Press: London, 1983.
(3) Asakura, S.; Oosawa, F. *J. Chem. Phys.* **1954**, *22*, 1255.
(4) Asakura, S.; Oosawa, F. *J. Polym. Sci.* **1958**, *33*, 183.
(5) Vrij, A. *Pure Appl. Chem.* **1976**, *48*, 471.
(6) Biben, T.; Hansen, J. P. *Europhys. Lett.* **1990**, *12*, 347.

0743-7463/92/2408-1919$03.00/0

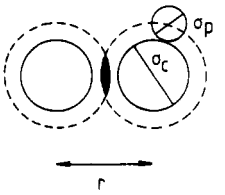

Figure 1. A pair of colloidal particles of diameter σ_c. The centers of the small (polymer) spheres, of diameter σ_p, are excluded from the dashed zone around each colloidal sphere. The solid volume shows the overlap of the depletion zones which occurs at small interparticle separations r.

were mixed with smaller deuterated PMMA spheres. The scattering length density ρ_m of the dispersion medium was adjusted, by altering the ratio of *cis*-decalin-h_{18} to octane-d_{18}, so that it approximately matched that of the larger hydrogenated spheres. The scattered intensity profile, measured under these conditions, contains information about the distribution of the smaller deuterated spheres. Although several experiments on binary colloidal suspensions have been reported in the literature,[7-9] these experiments are the first to study the structure of a fluid phase of an asymmetric mixture of purely repulsive colloidal particles.

2. Theoretical Background

The Potential of Mean Force. The problem of finding the effective pair potential between two large spheres in a mixture of smaller spheres has been considered by several authors.[5,10,11] Here we shall limit ourselves to the low-density limit in which the situation is clearer. Consider a binary mixture of hard spheres in which the two different sized species are labeled as i and j. The statistically averaged force between a pair of tagged particles of species i, say 1 and 2, when immersed in a dispersion containing *only* particles of species j defines the potential of mean force $V_{ii}(r_{12})$. The gradient of this effective potential $-dV_{ii}/dr_{12}$ gives the force between particles 1 and 2 after averaging over the equilibrium distribution of all the remaining j-type particles.[12] The relationship between the potential of mean force $V_{ii}(r_{12})$ and the tagged interparticle potential $u_{ii}(r_{12})$ can be seen clearly from the formally exact density expansion[13,14]

$$V_{ii}(r_{12}) = u_{ii}(r_{12}) - kT\sum_{m=1}^{\infty} n_j{}^m \xi_m(r_{12}) \tag{4}$$

where

$$\xi_1(r_{12}) = c_2(r_{12})$$

and

$$\xi_2(r_{12}) = d_3(r_{12}) + 2d_4(r_{12}) + {}^1/_2 d_5(r_{12})$$

The corresponding cluster integrals c_2, $d_3 \ldots d_5$ are given in a diagrammatic form in Figure 2. The first-order term in the density expansion, eq 4, contains the integral

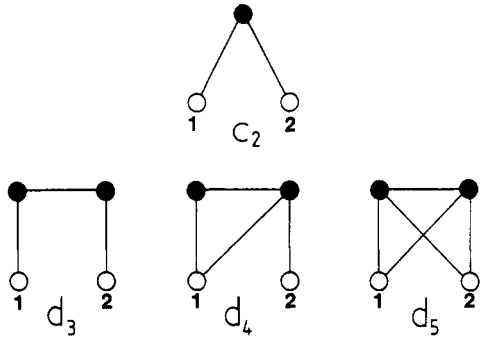

Figure 2. Irreducible cluster integrals c_2, d_3, d_4, and d_5. Each bond represents the Mayer f-function of the particles i and j associated with the bond connecting circles i and j. The value of a diagram is defined by an integration of the corresponding product of f-functions over the positions of the bath particles represented by the unlabeled black circles. The result is a function of the coordinates of the tagged particles labeling the white circles.

$$c_2(r_{12}) = \int f_{13} f_{23}\, d\mathbf{r}_3 \tag{5}$$

where particle 3 is a j-type sphere. The Mayer f-function is related to the interparticle potential $u(r)$ by the expression

$$f(r) = \exp^{-u(r)/kT} - 1 \tag{6}$$

which for the hard-sphere interaction (eq 1) becomes

$$f(r_{ij}) = \begin{cases} -1 & r < \sigma_{ij} \\ 0 & r > \sigma_{ij} \end{cases} \tag{7}$$

Consequently the cluster integral $c_2(r_{12})$ represents the volume common to two spheres of radius σ_{ij} separated by a distance r_{12}

$$c_2(r_{12}) = \begin{cases} \frac{4}{3}\pi\sigma_{ij}{}^3\left[1 - \frac{3}{4}\left(\frac{r_{12}}{\sigma_{ij}}\right) + \frac{1}{16}\left(\frac{r_{12}}{\sigma_{ij}}\right)^3\right] & 0 < r_{12} < 2\sigma_{ij} \\ 0 & r_{12} > 2\sigma_{ij} \end{cases} \tag{8}$$

The complexity of the higher order terms (ξ_2 and above) in the density expansion increases rapidly with order, so that their evaluation becomes a difficult (and in general an analytically insoluble) problem. Only in a few, rather unique, cases are the highest order terms known explicitly. If, for example, the bath spheres are perfectly permeable to each other, i.e. $\sigma_{jj} = 0$, then all the terms $\xi_m(r_{12})$ with $m \geq 2$ are zero. To see this, consider the integral $d_3(r_{12})$ which can be written as

$$d_3(r_{12}) = -\int d\mathbf{r}_3 d'_3(r_{12}, r_{13}, r_{23}) \tag{9}$$

where

$$d'_3(r_{12}, r_{13}, r_{23}) = -\int d\mathbf{r}_4 f_{13} f_{34} f_{24}$$

For hard spheres d'_3 is the volume common to three spheres, two of radius σ_{ij} and one of radius σ_{jj}, which for $\sigma_{jj} = 0$ is zero. Similar arguments apply to the other cluster integrals so that overall ξ_2 is zero. Physically this corresponds to a situation in which the bath spheres are behaving ideally so that the unbalanced osmotic pressure driving the tagged particles together must be linear in the number density n_j. In the context of the AO model, in which the spheres i and j are identified with the colloid and polymer species, respectively, the resulting effective potential is given by eqs 4 and 8 (together equivalent to eq 3).

(7) Duits, M. H. G.; May, R. P.; Vrij, A.; De Kruif, C. G. *J. Chem. Phys.* **1991**, *94*, 4521.
(8) Hanley, H. J. M.; Straty, G. C.; Lindner, P. *Physica A* **1991**, *174*, 60.
(9) Bartlett, P.; Ottewill, R. H. *J. Chem. Phys.* **1992**, *96*, 3306.
(10) Henderson, D. *J. Colloid Interface Sci.* **1988**, *121*, 486.
(11) Attard, P. *J. Chem. Phys.* **1989**, *91*, 3083.
(12) Chandler, D. *Introduction to Modern Statistical Mechanics*; Oxford University Press: Oxford, 1987.
(13) Hansen, J. P.; McDonald, I. R. *Theory of Simple Liquids*; Academic Press: London, 1986.
(14) Barker, J. A.; Henderson, D. *Rev. Mod. Phys.* **1976**, *48*, 587.

The situation for an asymmetric hard-sphere mixture, for which $\sigma_{jj} \neq 0$, is however a little different. The terms $\xi_m, m \geq 2$, are now nonzero so that the conventional depletion expression

$$V_{ii}(r_{12}) = u_{ii}(r_{12}) - kTn_j c_2(r_{12}) \tag{10}$$

remains valid only in the limit of a low density of j-spheres where the higher order terms may be ignored. Note that the original form for this expression[3,4] was derived with the implicit assumption that $\sigma_i \gg \sigma_j$. As is evident from above, this restriction is not strictly necessary. For the case in which the tagged (A) spheres are larger than the remaining (B) spheres, the effective potential may be written as

$$\frac{V_{AA}(R)}{kT} = \begin{cases} \infty & \text{for } R < 1 \\ -\dfrac{\phi_B}{2\gamma^3}[R^3 - 3R(\gamma+1)^2 + 2(\gamma+1)^3] & \text{for } 1 < R < (1+\gamma) \\ 0 & \text{otherwise} \end{cases} \tag{11}$$

where R is the scaled interparticle separation r/σ_{AA}, ϕ_B is the volume fraction of the smaller (B) spheres, and γ is the diameter ratio σ_{BB}/σ_{AA} (i.e. $\gamma \leq 1$). Conversely the effective potential between a pair of small (B) spheres in a dispersion of large (A) spheres is given by the expression

$$\frac{V_{BB}(R')}{kT} = \begin{cases} \infty & \text{for } R' < 1 \\ -\dfrac{\phi_A}{2}[R'^3\gamma^3 - 3R'\gamma(\gamma+1)^2 + 2(\gamma+1)^3] & \text{for } 1 < R' < \left(1+\dfrac{1}{\gamma}\right) \\ 0 & \text{otherwise} \end{cases} \tag{12}$$

where now R' is r/σ_{BB} and ϕ_A is the volume fraction of the large spheres. Inspection of eqs 11 and 12 reveals that if γ is small, the effective potential between the large spheres is strongly attractive (with a minimum at $R = 1$ of $-3kT \cdot \phi_B/2\gamma$) and short-ranged while conversely the small sphere potential is long-ranged but shallow (with a minimum of $-\phi_A kT$ at $R' = 1$).

Finally it should be noted that the expression for the potential of mean force (eq 4) is only valid in the limit of vanishingly small tagged particle densities. In general the effective potential will be a function of the density of the tagged species. Consequently the conventional treatment of polymer-induced clustering[15] in which eq 3 is used as a density-independent potential in a one-component model is a rather severe approximation. While the density dependence of the depletion potential is minimized if, as is normally the case for polymer–colloid mixtures, the depleted particles are considerably smaller than the tagged particles (i.e. $\sigma_{jj} \ll \sigma_{ii}$), recent simulation results[16] still show that the Asakura–Oosawa potential results in an overestimation of the tendency of the colloidal particles to cluster.

Second Virial Coefficients. The effect on the microstructure of the depletion potential can be gauged by considering the corresponding second virial coefficient b, defined as

$$b = 2\pi \int_0^\infty [1 - \exp^{-V(r)/kT}] r^2 \, dr \tag{13}$$

For the potentials given by eqs 11 and 12, this integral is, in general, nonanalytic. However, considering the densities at which eqs 11 and 12 are valid, the second virial coefficients may be approximated, to first order, by the expressions

$$\frac{b_{AA}(\phi_B)}{b_A} \approx 1 - \frac{\phi_B}{8}(12 + 15\gamma + 6\gamma^2 + \gamma^3) \tag{14}$$

$$\frac{b_{BB}(\phi_A)}{b_B} \approx 1 - \frac{\phi_A}{8\gamma^3}(1 + 6\gamma + 15\gamma^2 + 12\gamma^3) \tag{15}$$

where b_{AA} (b_{BB}) is the effective virial coefficient between a pair of A (B) spheres in a dispersion of B (A) spheres and b_A (b_B) is the corresponding hard-sphere result $4\phi_A$ ($4\phi_B$). Clearly the effect of the depletion interaction is to reduce the second virial coefficient of both the large and small spheres. Note however that the reduction is much more marked for the smaller spheres. Indeed in the limit of a very asymmetric mixture, where γ approaches zero, while the normalized second virial coefficient of the large spheres remain finite at $1 - 3\phi_B/2$ the value for the smaller spheres diverges as $1 - (\phi_A/8\gamma^3)$. Evidently the depletion interactions in a binary mixture are most strongly manifested among the smaller sized component. As we shall show in the next section, this conclusion remains valid at densities where eqs 11 and 12 are no longer applicable.

The Percus–Yevick Approximation. The equations derived above are strictly only valid in the limit of small dispersion densities. At higher densities a more convenient (and accurate) route to the structural correlations present in a binary mixture is via an integral equation approach, such as the Percus–Yevick closure.[13] While the PY approximation, as applied to hard spheres, is known to be quantitatively in error at very high densities,[13] and possibly also at extreme size ratios,[17] the solutions are at least qualitatively reliable and mathematically simple. Since our primary aim here is physical insight, we shall limit our discussion to the PY level although, as pointed out by Biben and Hansen,[17] more accurate self-consistent approaches may be required to understand quantitatively the structure of highly asymmetric mixtures (where $\gamma \to 0$).

In general the pair structure of a two-component mixture may be described by three partial pair distribution functions $g_{ij}(r)$ (i,j = A or B) and their Fourier transforms, the partial structure factors $S_{ij}(q)$. The functions $S_{ij}(q)$ can be related to $\tilde{C}_{ij}(q)/(n_i n_j)^{1/2}$, the Fourier transform of the Ornstein–Zernike direct correlation function $c_{ij}(r)$, by the matrix equation

$$S(q)\,[I - \tilde{C}(q)] = I \tag{16}$$

where I is the unit matrix and $S(q)$ and $\tilde{C}(q)$ are 2×2 matrices with the elements $S_{ij}(q)$ and $\tilde{C}_{ij}(q)$, respectively. Baxter[18] has shown that if the direct correlation function $c_{ij}(r)$ can be assumed to vanish when $r > {}^1/_2(\sigma_{ii} + \sigma_{jj})$, then the matrix $I - \tilde{C}(q)$ may be factorized as follows

$$I - \tilde{C}(q) = \tilde{Q}^T(-q)\tilde{Q}(q) \tag{17}$$

The explicit form of the matrix elements $\tilde{Q}_{ij}(q)$, for a multicomponent system of (additive) hard-spheres, has been given by Vrij.[19] With these results the matrix $I - \tilde{C}(q)$ may be analytically inverted and the partial structure factors obtained. Here rather than quote the full result we concentrate on the $q = 0$ limit. It is straightforward to show that the limiting PY forms of the partial structure

(15) See, for example: Gast, A. P.; Hall, C. K.; Russel, W. B. *Faraday Discuss. Chem. Soc.* **1983**, *76*, 189.
(16) Meijer, E. J.; Frenkel, D. *Phys. Rev. Lett.* **1991**, *67*, 1110.
(17) Biben, T.; Hansen, J. P. *Phys. Rev. Lett.* **1991**, *66*, 2215.
(18) Baxter, R. J. *J. Chem. Phys.* **1970**, *52*, 4559.
(19) Vrij, A. *J. Chem. Phys.* **1979**, *71*, 3267.

factors in a binary mixture of hard spheres are

$$\frac{(1+2\phi)^2}{(1-\phi)^4}S_{AA}(0) = 1 + 2\phi_B F_{BB} + \phi_A\phi_B F_{AB}^2 + \phi_B^2 F_{BB}^2 \quad (18)$$

$$\frac{(1+2\phi)^2}{(1-\phi)^4}S_{BB}(0) = 1 + 2\phi_A F_{AA} + \phi_A\phi_B F_{BA}^2 + \phi_A^2 F_{AA}^2 \quad (19)$$

$$\frac{(1+2\phi)^2}{(1-\phi)^4}S_{AB}(0) = -(\phi_A\phi_B)^{1/2}\{\phi_A F_{AA}F_{AB} + \phi_B F_{BB}F_{BA}\} \quad (20)$$

where, with i, j = A or B

$$(1-\phi)^2 F_{ij}\left(\frac{\sigma_{ii}}{\sigma_{jj}}\right)^{3/2} = \left(1 + 3\frac{\sigma_{ii}}{\sigma_{jj}}\right)(1-\phi) + 3\eta\sigma_{ii}$$

and

$$\phi = \phi_A + \phi_B$$

$$\eta = \frac{\phi_A}{\sigma_{AA}} + \frac{\phi_B}{\sigma_{BB}}$$

An expansion of these expressions in powers of ϕ_A and ϕ_B gives identical results for the second virial coefficients to those found above (eqs 14 and 15).

The asymmetry in the structure of a mixture of very differently sized spheres is seen clearly from eqs 18–20. In the limit as γ approaches zero the self-structure factors reduce to the expressions

$$\lim_{\gamma\to 0} S_{AA}(0) = (1-\phi_A)^2\left[\frac{1-\phi_A+2\phi_B}{1+2\phi_A+2\phi_B}\right]^2 \quad (21)$$

$$\lim_{\gamma\to 0} S_{BB}(0) = \frac{\phi_A\phi_B}{\gamma^3}\left[\frac{1-\phi_A+2\phi_B}{1+2\phi_A+2\phi_B}\right]^2 \quad (22)$$

Inspection of eqs 21 and 22 reveals, as first pointed out by Biben and Hansen,[6] that the small sphere structure factor diverges at small q as the size ratio $\gamma \to 0$ while the large sphere structure factor remains finite. Hence, as expected from the depletion arguments, the distribution (reflected by the long wavelength density fluctuations $S_{ii}(0)$) of the two differently sized particles is very different. The deviation from a purely random mixture of spheres is most readily seen for the smaller species where there is a tendency toward particle clustering. On the contrary, within the Percus–Yevick approximation, the low q limit of the structure factor of the large spheres is much closer to the one-component PY result $(1-\phi_A)^4/(1+2\phi_A)^2$. Note that this is only true at the PY level. Other integral equations (see ref 17) give different results for the low q limiting form of the large sphere structure factor in a hard-sphere mixture.

Small-Angle Neutron Scattering. The differential cross section for neutrons scattered from a unit volume of a binary colloidal dispersion containing spherical particles A and B can be expressed as

$$\frac{d\Sigma}{d\Omega}(q) = n_A P_A^2(q)S_{AA}(q) + 2(n_A n_B)^{1/2}P_A(q)P_B(q)S_{AB}(q) + n_B P_B^2(q)S_{BB}(q) \quad (23)$$

where n_A and n_B are the particle number densities, P_A and P_B are the single particle scattering amplitudes, S_{AA}, S_{AB}, and S_{BB} are the three partial structure factors introduced above, and q is the usual scattering vector. The scattering amplitudes P_A, etc., are a function of the internal structure of the particles and the scattering length density (ρ_m) of the suspension medium (as well as the scattering vector q). By an appropriate manipulation of ρ_m the partial intensities can be extracted from the measured total cross section. For details of this procedure see ref 9. In particular if ρ_m is chosen so that the single particle scattering from the large spheres is negligible, i.e. $P_A(q) \approx 0$, then eq 23 becomes

$$\frac{d\Sigma}{d\Omega}(q) \sim n_B P_B^2(q)S_{BB}(q) \quad (24)$$

and the measured intensity reflects only the small sphere microstructure.

3. Experimental Section

Sample Details. The experiments were carried out with mixed nonaqueous suspensions of hydrogenated and deuterated poly(methyl methacrylate) (PMMA) latices. The uniform spherical particles were prepared[20] by a dispersion polymerization of either hydrogenated or deuterated methyl methacrylate in the presence of a comb copolymer of poly(12-hydroxystearic acid) (PHS) and poly(glycidyl methacrylate–methyl methacrylate). The latex was purified by repeated centrifugation, decanting the supernatant and replacing it with fresh *cis*-decalin-h_{18} each time. The resulting particles have a composite structure, with a core of either hydrogenated or deuterated PMMA and a grafted stabilizing layer of hydrogenated PHS. One-component suspensions of these particles have been studied extensively in the last few years (for a short review see ref 21) and these experiments have established that the interparticle potential is predominantly repulsive and closely approximated by a hard-sphere interaction. There is no evidence for an attractive component in the pair potential.

The respective number averaged diameters of the hydrogenated and deuterated particles were determined from dynamic light scattering measurements as 315 ± 2 and 97 ± 2 nm giving a diameter ratio of approximately 0.31. The corresponding size polydispersities (standard deviation divided by the mean) were found from electron micrographs to be 0.05 ± 0.01 and 0.13 ± 0.01.

Stock dispersions of each latex were made in *cis*-decalin-h_{18}. Because the density of the composite core-shell particle was not known precisely, the effective volume fraction [volume occupied by the composite particles/total sample volume] could not be determined reliably from the dispersion weight fraction. Here, as in previous work,[21] an alternative approach based on the observation of the position of the fluid–solid phase transition was adopted. First, accurate values for the particle core volume fractions ϕ_c were calculated from the measured suspension dry weight fraction using literature values for the densities of hydrogenated (1.188 g cm^{-3}) and an estimated value for deuterated PMMA (1.282 g cm^{-3}). Then the particle core volume fraction at which colloidal crystallization first occurred (the freezing transition) was identified with value found, from computer simulation, for hard spheres, namely $\phi_f = 0.494$. All other core volume fractions were then scaled by the same factor to give effective hard-sphere volume fractions ϕ_{hs}. For the large (hydrogenated) latex the ratio ϕ_{hs}/ϕ_c was found to be 1.193 corresponding to an effective hard-sphere radius approximately 9 nm larger than the core and in close agreement with estimates for the thickness of the PHS layer. The smaller (deuterated) particles were sufficiently polydisperse so that the fluid–solid phase transition was suppressed. Consequently, in the absence of freezing data, the effective hard-sphere volume fraction of the smaller particles was estimated by assuming the ratio ϕ_{hs}/ϕ_c was unchanged from that found for the hydrogenated particles. This gave a better agreement between the scattering data and theory than the scaling previously used.[9]

(20) Antl, L.; Goodwin, J. G.; Hill, R. D.; Ottewill, R. H.; Owens, S. M.; Papworth, S. *Colloid Surf.* **1986**, *17*, 67.

(21) Pusey, P. N.; Van Megen, W.; Underwood, S. M.; Bartlett, P.; Ottewill, R. H. *Physica A* **1991**, *176*, 16.

Table I. Partial Volume Fractions and Compositions of the Experimental Samples[a]

sample	ϕ_A	ϕ_B	n_B/n_A
1	0.455	0.017	1.4
2	0.455	0.025	2.1
3	0.452	0.034	2.8
4	0.451	0.051	4.3
5	0.451	0.068	5.7

[a] Here A labels the larger and B the smaller sized colloidal spheres. The dispersion medium was 12.9%, by weight, octane-d_{18} and 87.1% *cis*-decalin-h_{18}.

Table II. Coherent Scattering Length Densities (ρ)

material	$\rho/10^{-6}$ Å^{-2}	material	$\rho/10^{-6}$ Å^{-2}
PMMA-*h*	1.07	*cis*-decalin-h_{18}	−0.03
PMMA-*d*	7.02	octane-d_{18}	6.42
PHS-*h*	−0.06		

The two stock dispersions were then mixed thoroughly together with an accurately weighed quantity of octane-d_{18} to give bimodal dispersions with a fixed medium scattering length density of $\rho_m \sim 0.87 \times 10^{-6}$ Å^{-2} (12.9% by weight octane-d_{18}). Under these contrast conditions the small (deuterated) spheres scatter much more intensely then the larger (hydrogenated) spheres. The component volume fractions and compositions of the five samples studied are summarized in Table I. The volume fraction of the large particles was held fixed at $\phi_A \approx 0.45$, sufficiently far below the freezing transition to ensure that the equilibrium state of all the samples studied was fluid.

SANS Measurements. The neutron scattering experiments were performed at the Institute Laue-Langevin, Grenoble, on the diffractometer D11. Colloidal dispersions were contained in 1 mm path length quartz cells thermostated at 25 °C. Measurements were made at a single sample–detector distance of 35.7 m which with an incident neutron beam wavelength of 10 Å gave an experimental q range of 1×10^{-3} to 8×10^{-3} Å^{-1}. The scattered intensity was collected on a two-dimensional detector and subsequently radially averaged. Corrections for sample attenuation, scattering from the quartz cell, and detector sensitivity were made by standard ILL procedures.

4. Results and Discussion

In these initial experiments contrast conditions were chosen so that the scattering from the smaller (deuterated) spheres dominated the measured intensity. This was readily achieved because of the very different scattering length densities of the hydrogenated (see Table II) and deuterated PMMA particle cores. However because of the composite core–shell nature of the system we used, the scattering from the larger spheres could not be completely eliminated at all wavevectors. At medium contrasts between the scattering length densities of the core and shell, complete destructive interference occurs only at certain unique values of q. For all other wavevectors the interference between neutrons scattered from the core and the shell is only partial and the scattered intensity remains small but finite. The choice of the medium contrast is thus within certain limits somewhat arbitrary. Here we chose a medium contrast of $\rho_m = 0.87 \times 10^{-6}$ Å^{-2} intermediate between the scattering length densities of the PHS shell and the hydrogenated PMMA core. In Figure 3, the averaged form factors of the small (◇) and large (○) spheres are presented. The curves have been scaled so that each corresponds to the scattering from a dispersion containing an equal number of particles. As can be seen from this figure the smaller deuterated particles scatter much more intensely over most of the q-range although at the lowest q values the scattering from the large spheres still remains appreciable. The solid lines show theoretical form factors which were calculated using core–shell models for the two particles determined from

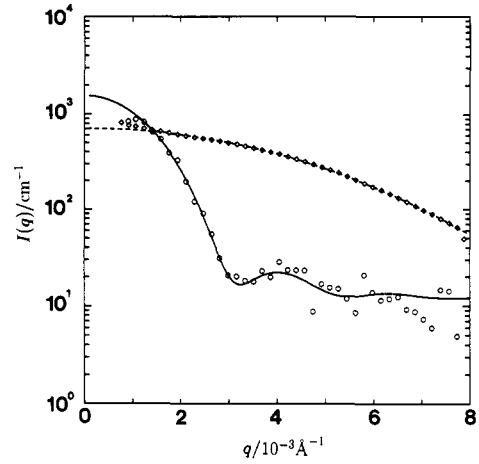

Figure 3. Measured form factors of the small, deuterated (◇) and large, hydrogenated (○) PMMA particles in a mixture of *cis*-decalin-h_{18} (87.1% by weight) and octane-d_{18} ($\rho_m = 0.87 \times 10^{-6}$ Å^{-2}). The solid lines are theoretical form factors calculated from the polydisperse core–shell model, described in the text, with the parameters listed in Table III. The curves have been scaled so that the intensity levels are for the same particle number density.

Table III. Model Description of the Particle Form Factors

quantity[a]	species A[b]	species B
$\rho_c/10^{-6}$ Å^{-2}	1.07	7.02
$\bar{R}_c$/Å	1466	375
σ_c	0.04	0.16
$\rho_s/10^{-6}$ Å^{-2}	0.74	1.15
ΔR/Å	90.0	90.0

[a] The core has a scattering length density of ρ_c, a mean radius of $\bar{R}_c$, and a polydispersity of σ_c. The shell is of width ΔR and scattering length density ρ_s. [b] A and B are the large hydrogenated and small deuterated PMMA spheres, respectively.

a separate series of contrast variation experiments described elsewhere.[9] Instrumental resolution corrections were included following the procedures described by Ramakrishnan.[22] The models are summarized in Table III. Agreement is seen to be very satisfactory.

The intensities measured for the binary dispersions as a function of the volume fraction ϕ_B of small spheres are shown in Figure 4. In all these samples the medium contrast and the volume fraction of large spheres were fixed at $\rho_m = 0.87 \times 10^{-6}$ Å^{-2} and $\phi_A = 0.45$, respectively, while the small sphere volume fraction varied from between 0.017 (Figure 4A) to 0.068 (Figure 4E). This corresponds to a composition range $AB_{1.4}$ to $AB_{5.7}$. Qualitatively the most notable feature is that on raising the volume fraction of small spheres, the intensity scattered at small q increases drastically. This feature is connected with the increase, highlighted in section 2, of the low q limit of the partial structure factor $S_{BB}(q)$ as the small spheres increasingly cluster in the dispersion. Note that the low q scattering is large but finite so that while the correlation length increases it does not diverge. This is in line with visual observations of the samples which showed no signs of a macroscopic phase separation.

Although it can be seen that the qualitative features of the experimental data are in accord with the depletion arguments given in section 2, a complete comparison between experiment and theory requires model calculations for hard-sphere mixtures. Furthermore since, in practice, a colloidal dispersion always has a distribution

(22) Ramakrishnan, V. *J. Appl. Crystallogr.* **1985**, *18*, 42.

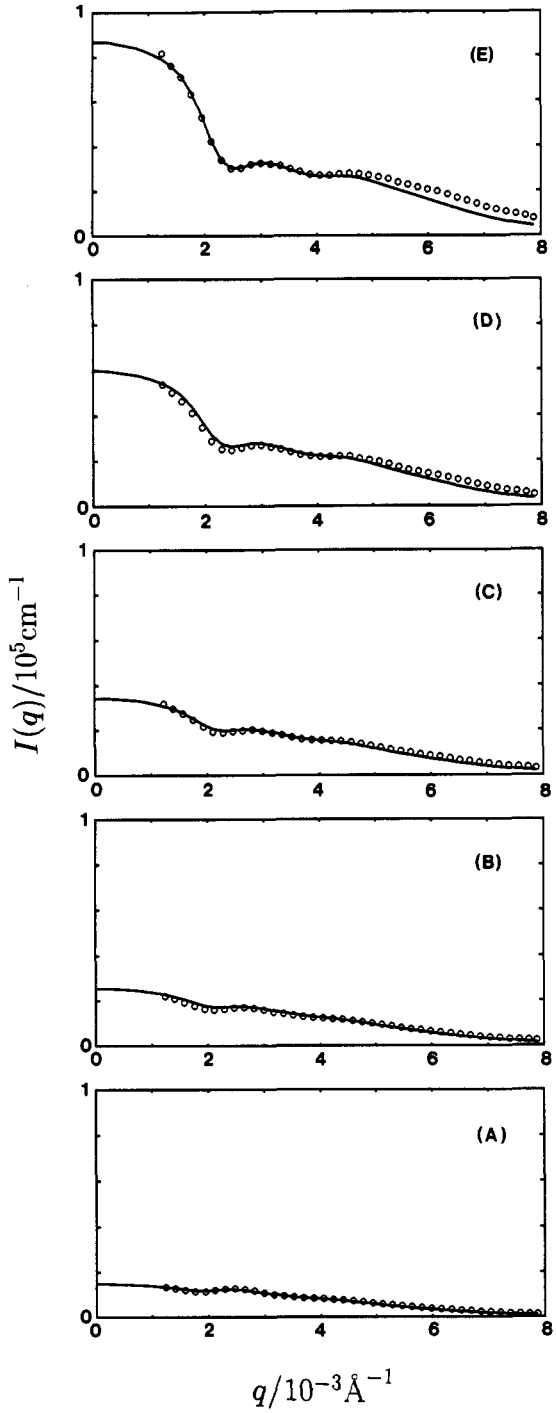

Figure 4. SANS intensity measured for bimodal dispersions of volume fractions $\phi_A = 0.45$ and (A) $\phi_B = 0.017$, (B) $\phi_B = 0.025$, (C) $\phi_B = 0.034$, (D) $\phi_B = 0.051$, and (E) $\phi_B = 0.068$. The dispersion medium was a mixture of 87.1% *cis*-decalin-h_{18} and 12.9% octane-d_{18} ($\rho_m = 0.87 \times 10^{-6}$ Å^{-2}). The solid lines are the results calculated from the hard-sphere model fits described in the text.

of particle sizes, polydispersity effects must also be considered. Polydispersity does not normally alter the qualitative features of the scattering but is essential if a quantitative comparison with theory is required. Fortunately for hard spheres the effect of a distribution of interaction diameters may be treated, at the PY level, using the expressions developed by Vrij.[19] Approximating the continuous distribution of large sphere diameters by a number (a_{max}) of closely spaced modes and a similar number (b_{max}) for the smaller particle distribution, eq 23 can be generalized as follows

$$\frac{d\Sigma}{d\Omega} = \sum_{i=1}^{a_{max}}\sum_{j=1}^{a_{max}}(n_i n_j)^{1/2}P_i P_j S_{ij} + 2\sum_{i=1}^{a_{max}}\sum_{k=1}^{b_{max}}(n_i n_k)^{1/2}P_i P_k S_{ik} + \sum_{k=1}^{b_{max}}\sum_{l=1}^{b_{max}}(n_k n_l)^{1/2}P_k P_l S_{kl} \quad (25)$$

for the case of a polydisperse binary dispersion. Here i and j label large particle modes while k and l represent the smaller sized modes. In terms of Vrij's analysis, the scattered intensity (eq 25) may be expressed, after some lengthy but straightforward manipulation, in terms of various angular averages of the distribution of scattering amplitudes (the $P_i(q)$ functions). These averages are calculated for our system using the form factor models given in Table III. The resulting intensities were then smeared by the procedure described by Ramakrishnan[22] in order to take the finite angular resolution of the diffractometer and the polychromaticity of the neutron beam into account. Model fits of the experimental intensity data were carried out by making a visual comparison, adjusting only a multiplicative scaling factor which was fixed at the same value for all samples, to obtain close agreement. This factor allowed for any systematic errors in the intensity calibration. The solid lines is Figure 4 depict the resulting fits. Comparison with the experimental data shows that the polydisperse hard-sphere model describes the measured intensities rather well. Calculations demonstrate that the low q scattering derived predominantly from the small deuterated particles with the larger hydrogenated spheres contributing less than 5% to the measured total intensity. A close inspection of Figure 4 reveals that the model intensities are slightly too low at high q values, which may suggest there are some errors in the modeling of the single particle form factors. However in view of the overall agreement between theory and experiment, obtained essentially with no sample-dependent fitting parameters, the results can be regarded as a confirmation of the validity of the hard-sphere model.

It is also interesting to compare the forms predicted by the hard-sphere model for the averaged partial structure factors which are defined as follows:

$$\bar{S}(q) = \frac{\sum_{i,j}(n_i n_j)^{1/2}P_i(q)P_j(q)S_{ij}(q)}{\sum_{i,j}(n_i n_j)^{1/2}P_i(q)P_j(q)} \quad (26)$$

The summation indices are limited to either only large or only small particle species to give a polydisperse generalization[9] of the two binary self-structure factors $S_{AA}(q)$ and $S_{BB}(q)$. Such averaged structure factors can be quantitatively compared with experiment. A selection of averaged structure factors is given in Figure 5 which illustrates the effect of varying the small sphere volume fraction. As already mentioned the two functions differ markedly in form, especially at low wavevectors. In particular, according to fluctuation theory

$$\lim_{q\to 0} S_{ii}(q) = \frac{\langle (n_i - \langle n_i \rangle)^2 \rangle}{\langle n_i \rangle} \quad (27)$$

where n_i is the local number density of i-type spheres and $\langle \ldots \rangle$ denotes an ensemble average. Consequently the low value for the small-q limit of the large sphere structure factor reflects the difficulty in creating local fluctuations in the packing of the large spheres. Correspondingly the large upturn in the small sphere structure factor as $q = 0$ is approached is connected with the clustering of the small spheres which generates regions of significantly different local number densities. It can also be seen that

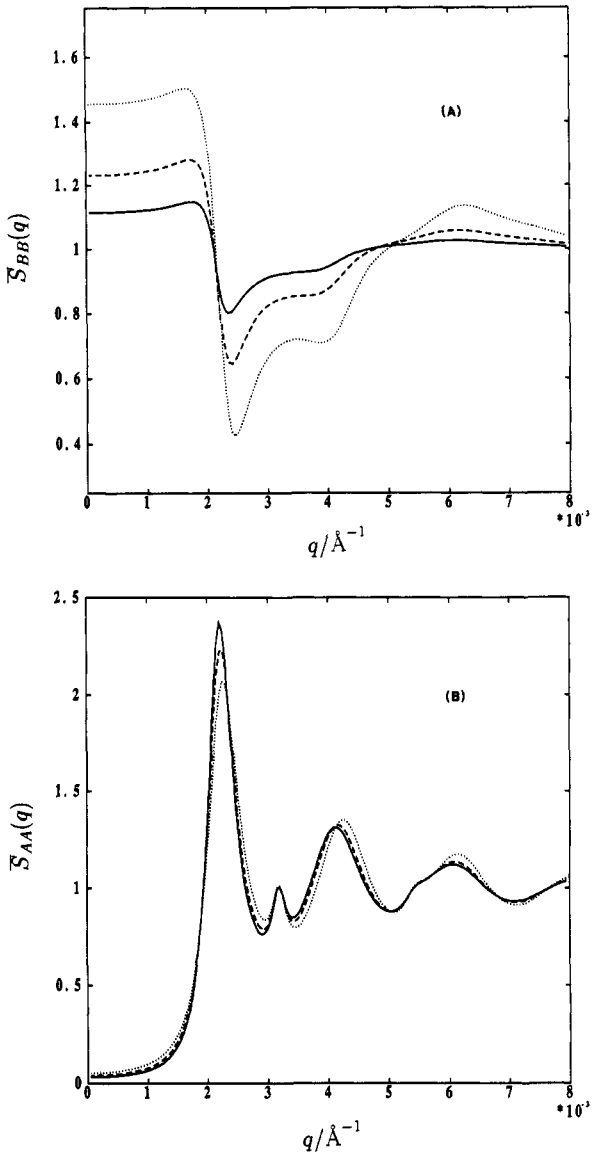

Figure 5. Averaged (A) small sphere and (B) large sphere partial structure factors for the fitted hard-sphere model shown in Figure 4. The full, dashed, and dotted lines refer to the dispersions of volume fractions ϕ_A = 0.45 and ϕ_B = 0.017, 0.034, and 0.068 respectively.

the peaks of the large sphere structure factor shift to larger momentum transfer with increasing small sphere content. This reflects the observation that the large spheres reside more closely, on average, in the mixtures.

Finally, we point out that although we have presented evidence for the clustering of small spheres in an additive hard-sphere dispersion, we see no sign of a macroscopic fluid phase separation. Indeed Lebowitz and Rowlinson[23] have shown that, within the PY approximation, an additive hard-sphere mixture remains completely miscible at all compositions and diameter ratios. The possibility that inaccuracies in the PY approximation may, at extreme size ratios, permit a fluid phase separation has been suggested recently by Biben and Hansen.[17] Using various self-consistent integral approximations, which are expected to be more accurate than the corresponding PY expressions, they have demonstrated that a hard-sphere mixture may phase separate at size ratios γ less than 0.2. This has been attributed to an enhanced depletion effect in these mixtures. Our binary dispersions at a size ratio of 0.31 are above this limit and thus might be expected to be miscible at all compositions. This should be contrasted with the very different phase behavior found in colloid–polymer mixtures.[2] In this case the nonadditivity in the colloid–polymer interaction diameter is known to strongly favor homocoordination and a fluid phase separation.

5. Conclusions

The present experiments demonstrate that the microstructure of a dispersion containing a mixture of very differently sized colloidal species can be understood in terms of depletion interactions. This model is appealing because of the physical insight it offers into the properties of binary dispersions. In particular the asymmetry in sizes of the two colloidal species results in very different forms for the effective attractive forces. While the interaction between the large spheres may be understood in terms of a short-ranged and deep effective potential, that for the smaller spheres is long-ranged and shallow. As a consequence, clustering is much more evident in the structure of the small spheres. This is confirmed by a small-angle neutron scattering study of the small sphere partial structure factor in a bimodal dispersion of nearly hard-sphere colloids.

Acknowledgment. We thank Dr. A. R. Rennie for his help in the SANS experiments and the Science and Engineering Research Council for support. Finally we are grateful to the Institute Laue-Langevin for the provision of neutron beam facilities.

Registry No. PMMA, 9011-14-7; *cis*-decalin, 493-01-6; octane, 111-65-9.

(23) Lebowitz, J. L.; Rowlinson, J. S. *J. Chem. Phys.* **1964**, *41*, 133.